Table S1: Coefficient of determination (R^2) stratified by year for minimum, average and maximum summer temperature offset models. We also indicated the number of time series on which the coefficient of determination was calculated for each year.

	2007	2008	2009	2010	2011	2012	2013	2014
# time series	2	2	8	92	90	113	100	147
Maximum	1.00	1.00	0.75	0.84	0.86	0.36	0.26	0.60
Average	1.00	1.00	0.93	0.94	0.95	0.86	0.72	0.72
Minimum	1.00	1.00	0.63	0.92	0.88	0.24	0.12	0.62

	2015	2016	2017	2018	2019	2020	2021	2022
# time series	219	70	321	763	482	759	730	478
Maximum	0.85	0.74	0.71	0.86	0.85	0.74	0.78	0.64
Average	0.89	0.83	0.79	0.86	0.85	0.81	0.82	0.78
Minimum	0.78	0.69	0.71	0.86	0.88	0.80	0.74	0.71

Table S2: Number of sensors at each height (cm). Note that one logger can have multiple sensors (e.g. TOMST TMS4).

Height (cm)	Number of sensors
0	276
1	62
2	311
5	232
10	106
12	47
15	870
20	39
25	28
30	2
50	100
100	518

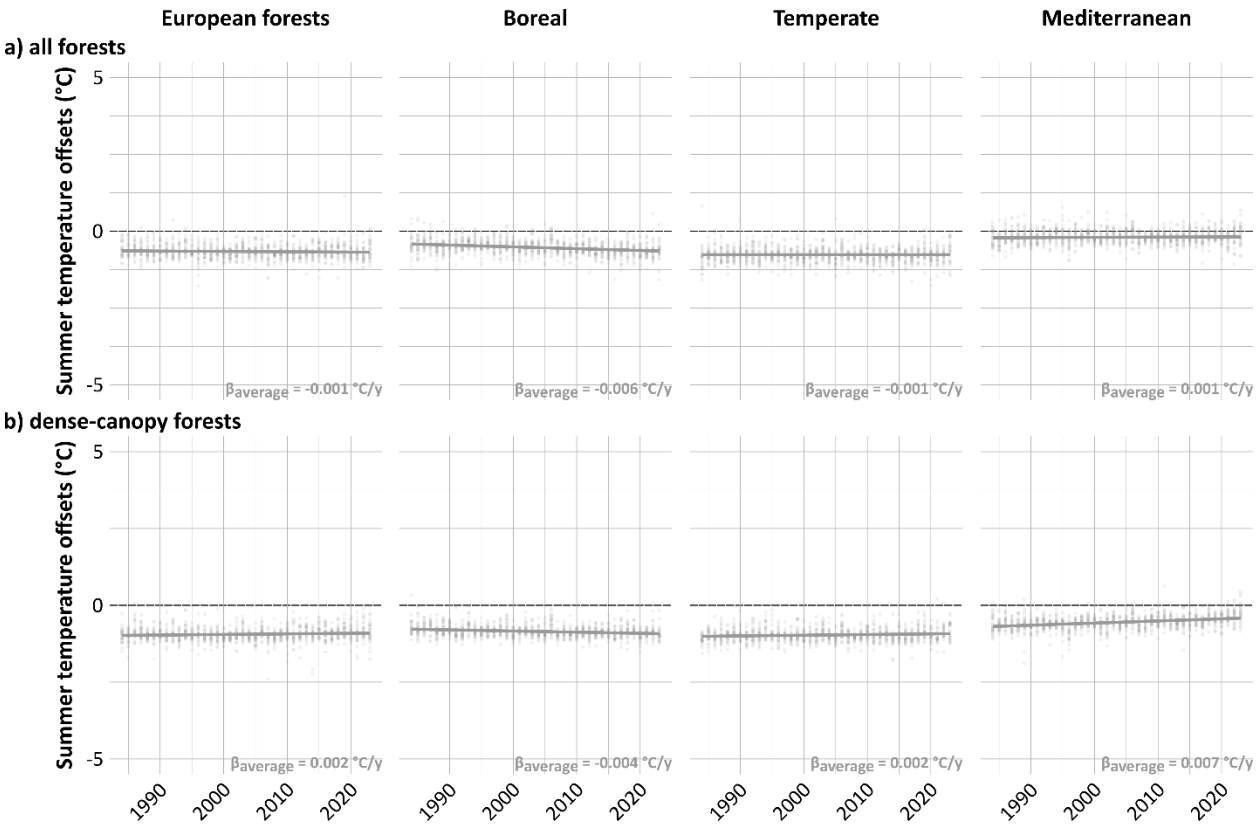

Fig. S1: Trends in thermal decoupling across European forests. These depict offsets (defined as microclimate minus macroclimate) from 1984 to 2023 for annual average summer temperatures across (a) all European forests and (b) across dense-canopy (NBR > 689) only. All are separated by the different biomes (boreal, temperate, and Mediterranean) as well. Dots represent partial residuals from linear mixed-effects models, illustrating variability across sites. Reported beta-values (i.e. slopes) indicate estimated rates of decoupling (°C yr^{-1}). Dots represent partial residuals from the linear mixed-effects models, illustrating variability across sites.

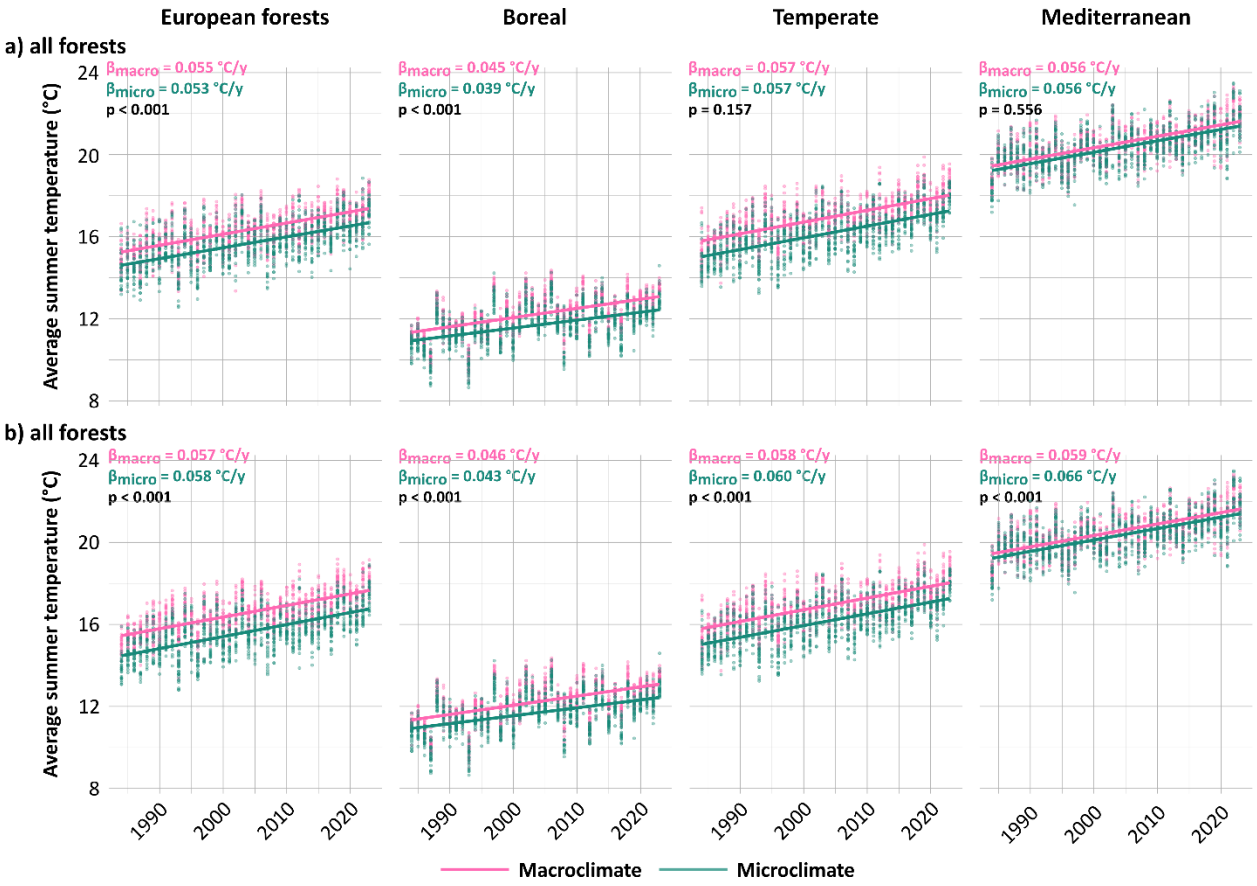

Fig. S2: Comparison between microclimate and macroclimate warming trends. Macroclimate (magenta) and microclimate (green) warming trends from 1984 to 2023 for annual average summer temperatures across (a) all European forests and (b) dense-canopy (NBR > 689) European forests. All are separated by the different biomes (boreal, temperate, and Mediterranean) as well. Reported beta-values (i.e. slopes) indicate estimated warming rates (°C yr^{-1}) for macroclimate (βmacro) and microclimate (βmicro); p-values test whether warming rates differ significantly between macroclimate and microclimate. Dots represent partial residuals from the linear mixed-effects models, illustrating variability across sites.

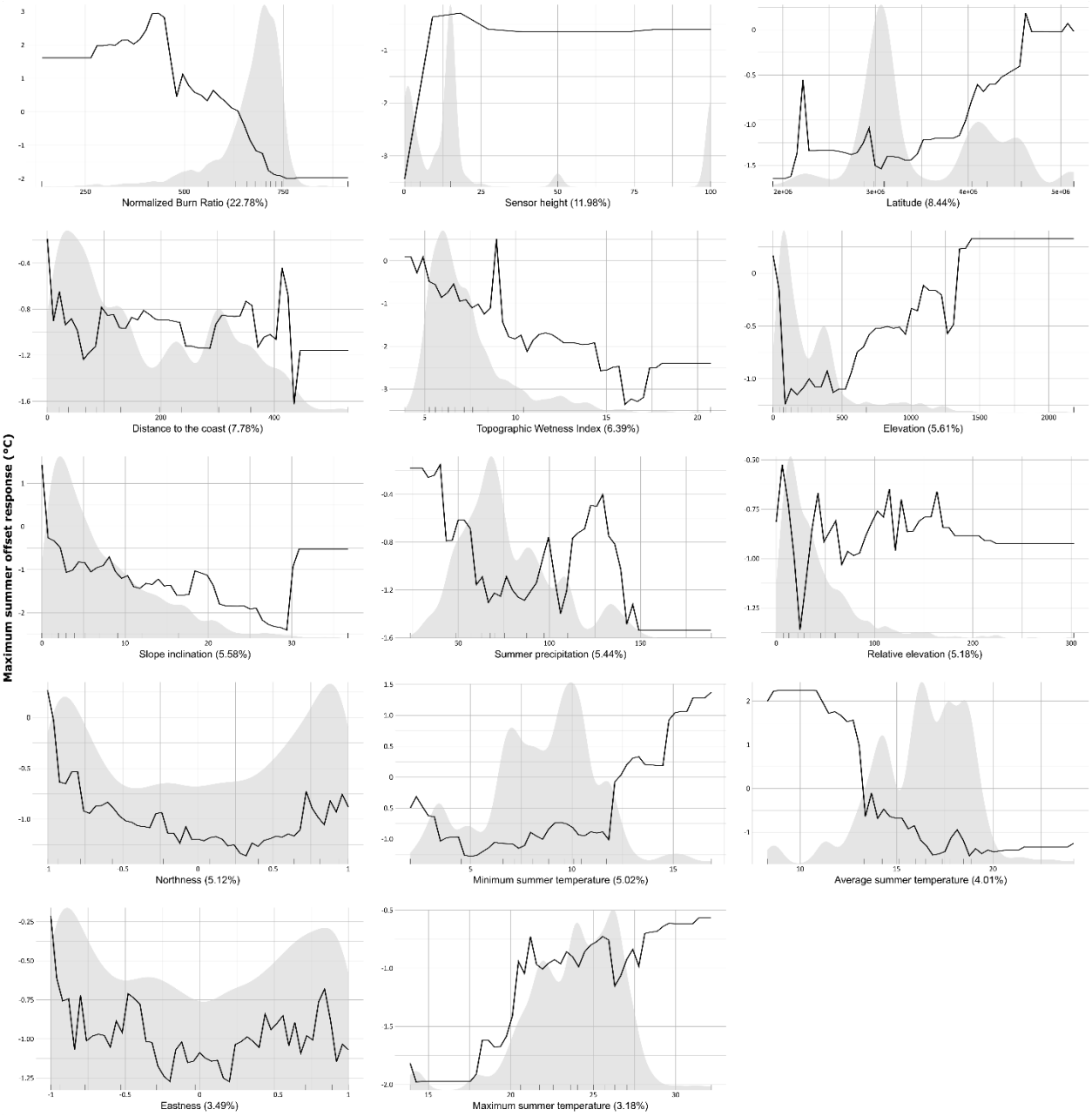

Fig. S3: Partial dependence plots of the response on the predictor variables in the boosted regression tree model for maximum summer temperature offsets. The plots indicate how much the response is affected by a certain predictor value, after accounting for the average effects of all other variables in the model. The relative importance of each predictor is reported between brackets. Gray backgrounds depict the distribution of the training data along that variable.

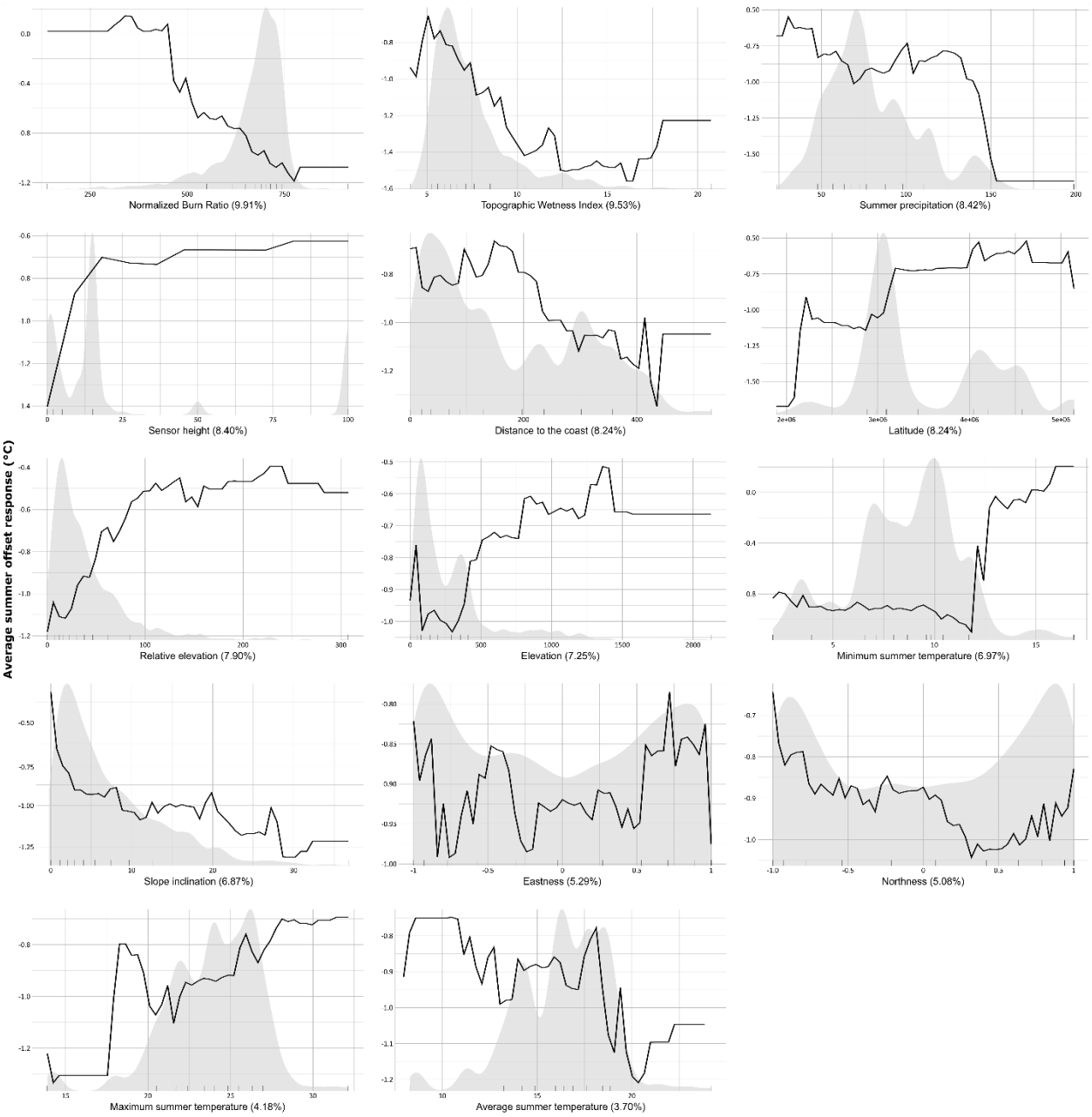

Fig. S4: Partial dependence plots of the response on the predictor variables in the boosted regression tree model for average summer temperature offsets. The plots indicate how much the response is affected by a certain predictor value, after accounting for the average effects of all other variables in the model. The relative importance of each predictor is reported between brackets. Gray backgrounds depict the distribution of the training data along that variable.

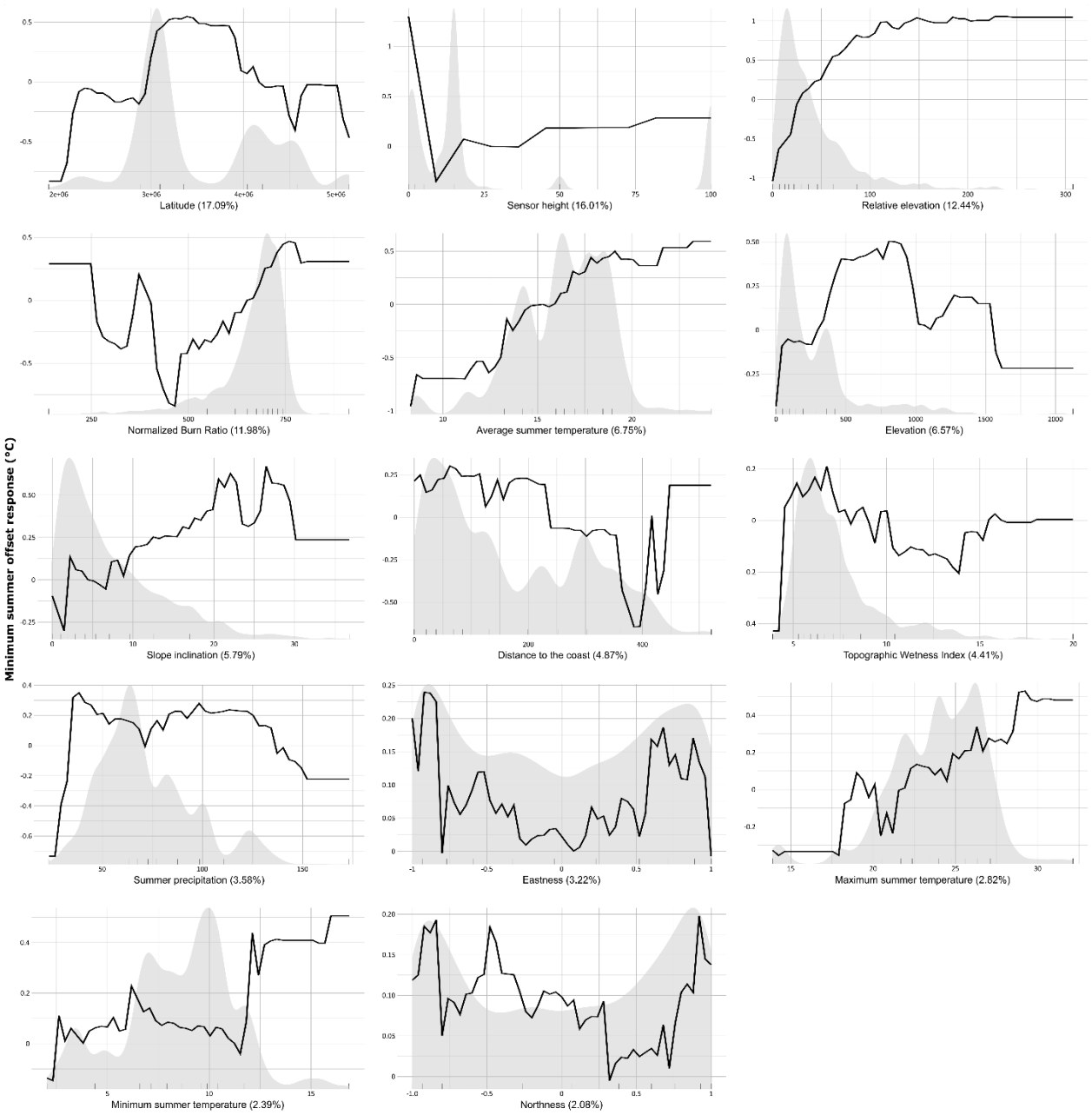

Fig. S5: Partial dependence plots of the response on the predictor variables in the boosted regression tree model for minimum summer temperature offsets. The plots indicate how much the response is affected by a certain predictor value, after accounting for the average effects of all other variables in the model. The relative importance of each predictor is reported between brackets. Gray backgrounds depict the distribution of the training data along that variable.

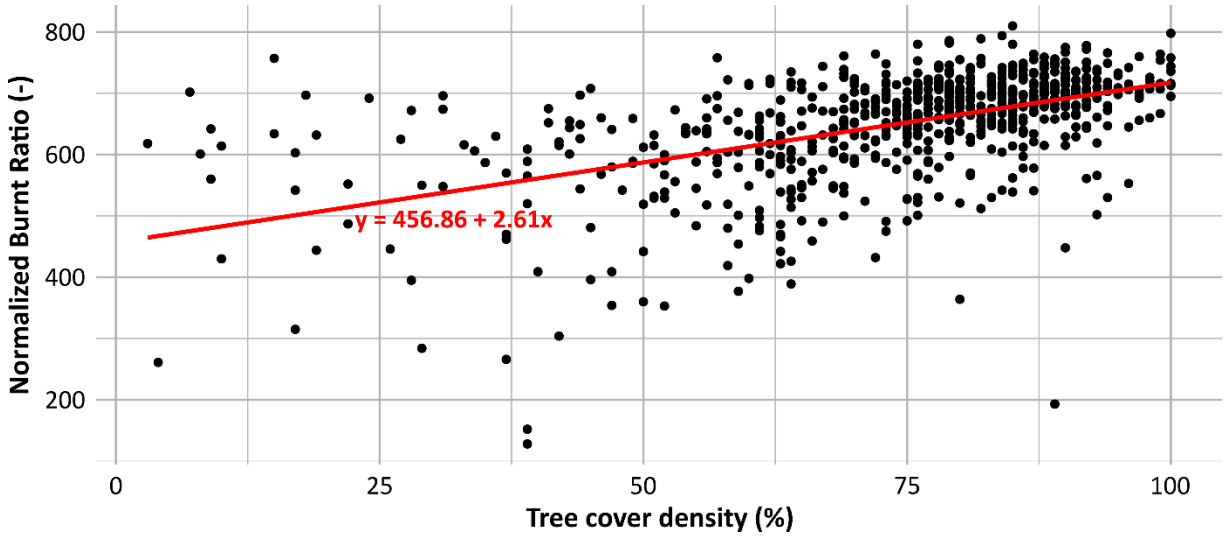

Fig. S6: Relationship between tree cover density (%) and normalized burnt ratio. Black points represent individual observations, and the red line shows the fitted linear regression, indicating a positive association between increasing tree cover density and normalized burnt ratio (y = 456.86 + 2.61x).

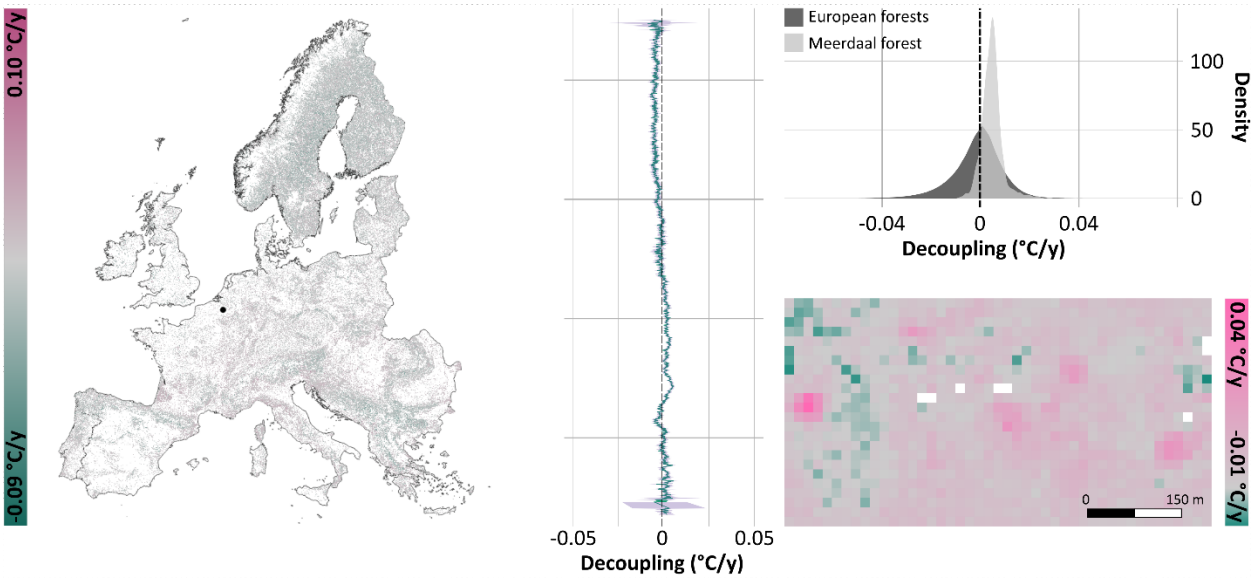

Fig. S7: Geospatial maps on the thermal decoupling between microclimate and macroclimate warming in European forests. Negative values indicate forest microclimate warms more slowly than the macroclimate outside the forest and positive values indicate faster warming inside than outside forests. Panels show decoupling across Europe at a spatial resolution of 30 m × 30 m (left), latitudinal variation (middle), and both the overall distribution of decoupling rates (density plot; right) together with a local case study highlighting the fine-scale heterogeneity present within a 1 km^2 area in a temperate mixed forest (Meerdaal forest, Belgium; represented as a black dot on the continental map). These are depicted for annual average summer temperatures (June–September).

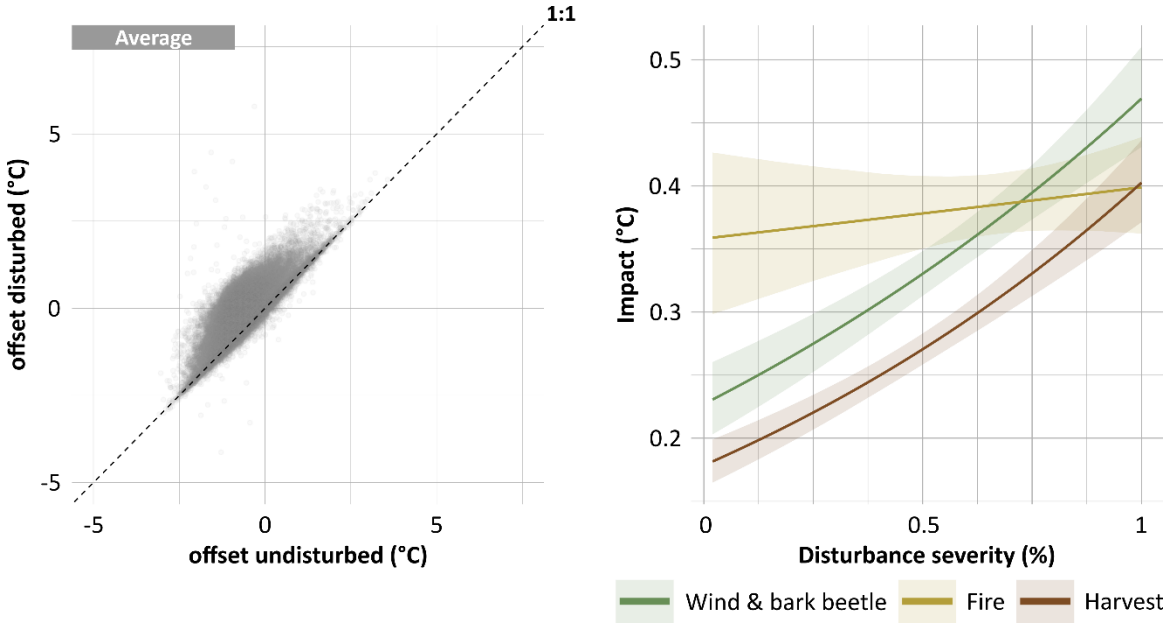

Fig. S8: Impact of disturbances on sub-canopy temperatures. (left) Change in annual average summer temperature offset after a disturbance event (n = 59,048). The offset following a disturbance event is plotted against the offset in the absence of disturbance. The dotted black line marks the 1:1 line, where disturbance causes no change in forest buffering capacity. For average temperatures, points above this line indicate a net loss in buffering capacitys. (right) Marginal effect plots showing the relationship between disturbance severity and its impact (= $offset_{disturbed} - offset_{undisturbed}$) on average temperature, with separate regression lines (with 95% confidence intervals) for each disturbance type (i.e., wind & bark beetle, fire, and harvest). Note that wind/bark beetle are grouped as their spectral signal could not be disentangled, and that it includes areas with post-disturbance salvage logging (removal of all biological legacies).

Fig. S9: Extrapolation maps. The percentage of quantitative variables for which the pixel lies outside the range of data covered by the training data. Pixels with high values indicate that the model has to extrapolate for many of the covariates for that specific pixel (i.e. due to missing in situ measurements).

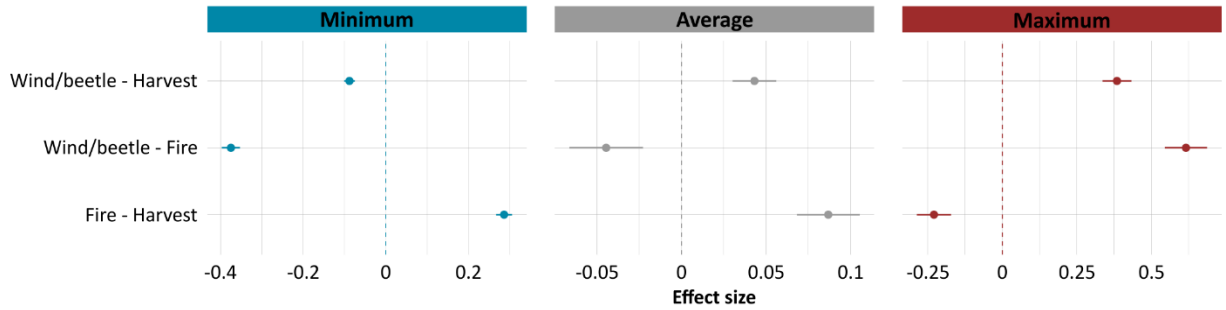

Fig. S10: Pairwise comparison of the impact of a disturbance event disturbance types (wind/bark beetle, fire, harvest), respectively, between wind/bark beetle-induced disturbances, fires, and harvest operations. A positive effect size of the comparison reflects more pronounced effects of the first disturbance type in the equation, whereas a negative effect size reflects the opposite result. Points and associated error bars correspond to posterior means and 95% highest posterior density intervals of the differences (of the standardized variables).